



BNL-209663-2018-JAAM

# Cross-section measurements and production of $^{72}\text{Se}$ with medium to high energy protons using arsenic containing targets

A. J. DeGraffenreid, C. Cutler

To be published in "Radiochimica Acta"

December 2018

Collider Accelerator Department  
**Brookhaven National Laboratory**

**U.S. Department of Energy**  
USDOE Office of Science (SC), Nuclear Physics (NP) (SC-26)

Notice: This manuscript has been authored by employees of Brookhaven Science Associates, LLC under Contract No. DE-SC0012704 with the U.S. Department of Energy. The publisher by accepting the manuscript for publication acknowledges that the United States Government retains a non-exclusive, paid-up, irrevocable, world-wide license to publish or reproduce the published form of this manuscript, or allow others to do so, for United States Government purposes.

## **DISCLAIMER**

This report was prepared as an account of work sponsored by an agency of the United States Government. Neither the United States Government nor any agency thereof, nor any of their employees, nor any of their contractors, subcontractors, or their employees, makes any warranty, express or implied, or assumes any legal liability or responsibility for the accuracy, completeness, or any third party's use or the results of such use of any information, apparatus, product, or process disclosed, or represents that its use would not infringe privately owned rights. Reference herein to any specific commercial product, process, or service by trade name, trademark, manufacturer, or otherwise, does not necessarily constitute or imply its endorsement, recommendation, or favoring by the United States Government or any agency thereof or its contractors or subcontractors. The views and opinions of authors expressed herein do not necessarily state or reflect those of the United States Government or any agency thereof.

# Cross-section measurements and production of $^{72}\text{Se}$ with medium to high energy protons using arsenic containing targets

Anthony J. DeGraffenreid<sup>1</sup>, Dmitri G. Medvedev<sup>1</sup>, Timothy E. Phelps<sup>2</sup>, Matthew D. Gott<sup>2</sup>, Suzanne V. Smith<sup>1</sup>, Silvia S. Jurisson<sup>2</sup>, Cathy S. Cutler<sup>1\*</sup>

<sup>1</sup>Collider Accelerator Department—Brookhaven National Laboratory—Upton, NY 11973, USA

<sup>2</sup>Department of Chemistry—University of Missouri—Columbia, MO 65211, USA

Received; accepted

As-72 generator / Positron emission tomography / Matched-pair / Theragnostic / Nuclear imaging / Therapy

**Abstract.** Experiments were performed to evaluate production of  $^{72}\text{Se}$ , parent radionuclide of the positron emitter  $^{72}\text{As}$ , at high energy at the Brookhaven Linac Isotope Producer (BLIP). Excitation functions for  $^{75}\text{As}(p, xn)^{72/75}\text{Se}$  in the 52-105 MeV energy range were measured by irradiating thin gallium arsenide (GaAs) wafers. Maximum cross section value for the  $^{nat}\text{As}(p, 4n)^{72}\text{Se}$  reaction in the energy range was  $103 \pm 9$  mb at  $52 \pm 1$  MeV. Production size GaAs and arsenic metal ( $\text{As}^\circ$ ) targets were irradiated with 136  $\mu\text{A}$  and 165  $\mu\text{A}$  beam current possessing an initial Linac energy of 117 MeV. A total of  $3.77 \pm 0.1$  GBq ( $102 \pm 3$  mCi) of  $^{72}\text{Se}$  was produced from a GaAs target at a calculated target entrance energy of 105.4 MeV, and  $13.8 \pm 0.3$  GBq ( $373 \pm 8$  mCi) of  $^{72}\text{Se}$  from an  $\text{As}^\circ$  target at a calculated incident energy of 49.5 MeV irradiated for 116.5 h and 68.9 h, respectively.

## 1. Introduction

Radioisotopes of yttrium,  $^{86}\text{Y}/^{90}\text{Y}$ , were the first theragnostic-pair suggested for imaging and radiotherapy<sup>[1]</sup>. Two radioarsenic isotopes,  $^{72/77}\text{As}$ , are another excellent example of a theragnostic-pair that can be used for imaging and radiotherapy. The PET radioisotope  $^{72}\text{As}$  (2.49 MeV  $\beta^+_{\text{Max}}$ ;  $t_{1/2}$ —26 h) and radiotherapeutic  $^{77}\text{As}$  (0.683 MeV  $\beta^+_{\text{Max}}$ ;  $t_{1/2}$ —38 h) have half-lives well suited for use with slow-localizing biomolecules (e.g., peptides and antibodies)<sup>[2]</sup>. The use of no-carrier added radioarsenic has been fairly limited while the use of carrier-added radioarsenic has been extensively reported<sup>[3-8]</sup>. Sparse reports on the use of no-carrier-added radioarsenic is in part due to its complicated redox chemistry. Under aerobic conditions, the reactive As(III) oxidizes to the unreactive As(V) state at low concentrations (1-5 mM)<sup>[9]</sup>. Additionally, the use of these radioisotopes as a theragnostic pair has been limited by the availability of  $^{72}\text{As}$ , which must be available to adequately assess  $^{77}\text{As}$  biodistribution.

No-carrier-added  $^{72}\text{As}$  can be obtained by irradiation of a natural or enriched germanium ( $\text{GeO}_2$  or  $\text{Ge}^\circ$ ) target via the  $^{70}\text{Ge}(n, \gamma)^{77}\text{Ge}$  ( $\beta^-$ ,  $t_{1/2}$ —11.2 h)  $\rightarrow$   $^{77}\text{As}$  reaction at a nuclear reactor<sup>[10-13]</sup>. Production of no-carrier added  $^{72}\text{As}$  requires the use of a charged particle beam (proton, deuteron, or alpha)<sup>[14-18]</sup>. Arsenic-72 can be produced in a small cyclotron using a low energy (10-20 MeV) proton beam via the  $^{nat}\text{Ge}(p, n)^{72}\text{As}$  or  $^{72}\text{Ge}(p, n)^{72}\text{As}$  reaction, but the half-life of  $^{72}\text{As}$  limits its availability to areas near the production facility. The thick target yield of  $^{72}\text{As}$  with a low-energy (18 MeV) proton beam is low, 92.8 MBq/ $\mu\text{Ah}$  (2.51 mCi/ $\mu\text{Ah}$  at 1  $\mu\text{A}$  for 1 h) and radioisotopic impurities such as  $^{71}\text{As}$  ( $t_{1/2}$ —65.3 h) and  $^{74}\text{As}$  ( $t_{1/2}$ —17.8 d) are more than 5%<sup>[15,19,20]</sup>. The use of an enriched  $^{72}\text{Ge}$  target may reduce the production of  $^{74}\text{As}$ , however, long-lived  $^{71}\text{As}$  will still be coproduced via the  $^{72}\text{Ge}(p, 2n)^{71}\text{As}$  reaction<sup>[21]</sup>. A more advantageous, and indirect route of  $^{72}\text{As}$  generation is possible through the production of its parent nuclide  $^{72}\text{Se}$  (EC;  $t_{1/2}$ —8.4 d)<sup>[14,22,23]</sup>. Due to the favorable parent/daughter half-life ratio, this route offers the benefit of providing  $^{72}\text{As}$  as needed at remote sites through a  $^{72}\text{Se}/^{72}\text{As}$  generator system.<sup>[22-26]</sup>

Several nuclear reactions have been previously evaluated for production of  $^{72}\text{Se}$ . These include proton spallation on alkali bromide targets (NaBr and RbBr) via the  $^{nat}\text{Br}(p, 2pxn)^{72}\text{Se}$  reaction, alpha bombardment of enriched  $^{70}\text{Ge}$ , via the  $^{70}\text{Ge}(^4\text{He}, 2n)$  reaction, or proton/deuteron bombardment of arsenic containing targets ( $\text{Cu}_3\text{Ge}-70$ ,  $\text{Cu}_3\text{As}$ ,  $\text{As}_2\text{O}_3$ ,  $\text{As}_2\text{S}_3$ , and  $\text{As}^\circ$ ) via the  $^{75}\text{As}(p, 4n)^{72}\text{Se}$  and  $^{75}\text{As}(d, 5n)^{72}\text{Se}$  reactions<sup>[14,22,27-36]</sup>. Long-lived radioimpurity,  $^{75}\text{Se}$  ( $t_{1/2}$ —119.8 d), is co-produced in some of these reactions but it decays to stable  $^{75}\text{As}$ . While  $^{75}\text{Se}$  reduces the specific activity, it does not generate a radionuclidic purity issue for  $^{72}\text{As}$  administration.

Ballard *et al.* reported on the production of  $^{72}\text{Se}$  by irradiation of a sodium bromide (NaBr; 51 g) target using protons in the 92 $\rightarrow$ 72 MeV energy window for a 10 h irradiation producing  $^{72}\text{Se}$  and  $^{75}\text{Se}$  at a rate of 0.328 GBq/ $\mu\text{A}$  (8.9 mCi/ $\mu\text{A}$ ) and 7.7 GBq/ $\mu\text{A}$  (208.0 mCi/ $\mu\text{A}$ ), a  $^{72}\text{Se}/^{75}\text{Se}$  ratio of 0.043, producing a total of 1.13 GBq (30.4 mCi)

$^{72}\text{Se}$  and 1.88 GBq (50.7 mCi)  $^{75}\text{Se}$ <sup>[37]</sup>. The authors suggested that even with significant co-production of  $^{75}\text{Se}$ , the  $^{72}\text{Se}$  product could be used to produce  $^{72}\text{As}$  generators for PET imaging applications, up to fifteen 0.37 GBq (10 mCi)  $^{72}\text{As}$  generators for a 50,000  $\mu\text{Ah}$  irradiation<sup>[22]</sup>.

The focus here is on the production of  $^{72}\text{Se}$  from natural arsenic for application in  $^{72}\text{Se}/^{72}\text{As}$  generators<sup>[14,38]</sup>. The excitation functions for the  $^{75}\text{As}(p, xn)$  reactions have been reported previously in the energy range from 3 to 45 MeV (Note: data by Levkovskij have been shown to be 18% too high)<sup>[14,39-41]</sup>. The cross section curve for the  $^{75}\text{As}(p, 4n)^{72}\text{Se}$  reaction shows an increase in cross section above 35 MeV reaching 86 mb at 45.2 MeV. Other radionuclides such as  $^{71,73,74,76}\text{As}$ ,  $^{71,73}\text{Se}$ ,  $^{68,69}\text{Ge}$ , and  $^{67,68}\text{Ga}$  were produced. However, they are not discussed here.

Cross section measurements for the production of long-lived selenium radioisotopes (i.e.,  $^{75}\text{Se}$ , and  $^{72}\text{Se}$ ) via the  $^{75}\text{As}(p, n)^{75}\text{Se}$ , and  $^{75}\text{As}(p, 4n)^{72}\text{Se}$  reactions in the energy range from 52 to 105 MeV protons are reported. The suitability of several arsenic containing targets for  $^{72}\text{Se}$  production were evaluated and discussed. Results of irradiations for thicker targets to produce larger quantities of radioselenium using GaAs, and As<sup>o</sup> targets are reported.

## 2. Experimental

### 2.1. General

**Caution!** Arsenic is toxic and therefore should be handled with care in a properly ventilated area with appropriate personal protective equipment. **Caution!** Radionuclides of arsenic, gallium, germanium, selenium, and sodium are produced and all work utilizing radioactive material was carried out using appropriate radiation safety procedures in facilities approved for such work. High-purity trace metal grade acids or bases (Sigma Aldrich—St. Louis, MO) were used as provided. High-purity hydrogen peroxide (Optima™; Fisher Scientific—Pittsburgh, PA), hydrochloric acid (Optima™) and nitric acid (TraceMetal™) were used without further purification. Any solutions used in processing were prepared using high-purity water produced in-house using a Millipore filtration unit (Merck Millipore—Billerica, MA). International radiochemistry guidelines published by Heinz et al. were followed in this manuscript<sup>[42]</sup>.

### 2.2. Cross section measurements

Theoretical calculations of the excitation functions for the  $^{75}\text{As}(p,4n)^{72}\text{Se}$  and  $^{75}\text{As}(p,n)^{75}\text{Se}$  nuclear reactions for proton energy up to 110 MeV were carried out using TALYS 1.4 and EMPIRE 3.1 (Rivoli) codes<sup>[43,44]</sup>. The Hybrid Monte-Carlo Simulation (HMS) option was used as the pre-equilibrium model in EMPIRE 3.1 calculations. The TALYS 1.4 code was used without modification. Experimental measurements of the cross sections were carried out using GaAs thin foils individually isolated in bolted aluminum capsules as previously described<sup>[45]</sup>. Aluminum monitor foils were used for beam current measurements in each experiment.

#### 2.2.1. Target design and irradiation parameters

Semiconductor quality (99.999%) GaAs wafers ( $d \times h = 2.0'' \times 0.005''$ ; 50.8 mm x 0.127 mm); AXT Inc.—Fremont, CA) were laser cut to a 1.0'' (25.4 mm) diameter at BNL. Thermal stability and decomposition temperature of the wafers were determined using a thermal gravimetric analyzer (TGA) on a Diamond TG/DGA unit (Perkin Elmer—Waltham, MA). All data were collected under a N<sub>2</sub> atmosphere and up to 1000 °C (**SFigure 1**).

High-purity aluminum foil (99.999%; Alfa Aesar—Ward Hill, MA) was placed in front of each GaAs wafer to measure the beam current via the well-known cross-section values for  $^{27}\text{Al}(p, x)^{22}\text{Na}$ <sup>[46-48]</sup>. The aluminum foil ( $d \times h = 1.0'' \times 0.001''$ ; 25.4 mm x 0.025 mm) and GaAs wafer were isolated in a bolted target can. To ensure close to ideal thermal contact between foil, wafer and target window, a well was individually machined into each target body (**Figure 1**). Cans were closed under a helium atmosphere in a laboratory glovebox.

Six irradiations were carried out with an incident LINAC energy of 117 MeV for 2 hours at 40  $\mu\text{A}$  to collect data at several energy points (**Table 1** and **Figure 2**). Aluminum slabs were used for energy degradation. Energy propagation calculations of protons through the target array elements (e.g., beamline windows, cooling water,

---

<sup>1</sup> The numbers for yields in GBq/uA (mCi/uA) were recalculated from the reported data using approach suggested in Otsuka and Takacs<sup>[37]</sup>.

degraders, and targets) were carried out using either Linear Energy Transfer (LET) software LETCalc. or the Stopping and Range of Ions in Matter (SRIM)<sup>[49,50]</sup>.

### 2.2.2. *Target dissolution and data analysis*

The quantities of the radionuclides produced were determined by dissolving the foils separately and assaying the resulting solutions by HPGe. In a typical experiment, the irradiated target was transferred to a hot cell within 1-2 hours after end of bombardment (EOB), the target can opened, and the target transferred to a glass beaker and dissolved.

The GaAs wafer was dissolved in a 1:1 mixture of concentrated nitric acid and 30% H<sub>2</sub>O<sub>2</sub>, quantitatively transferred to a 100 mL volumetric flask with 0.1 M HNO<sub>3</sub> and brought to volume. A precise aliquot of the resulting solution was extracted for analysis. Aliquots ranged from 20-75  $\mu$ L and 0.5-1 mL for initial, and decayed time points, respectively. Aluminum foils were dissolved in a few mL of concentrated HCl and a few drops of concentrated HNO<sub>3</sub>, quantitatively transferred to a 50 mL volumetric flask with 18 M $\Omega$  H<sub>2</sub>O, brought to volume, and a 1 mL sample removed from each for analysis. All solutions were diluted to 3 mL and assayed (n = 2) shortly after dissolution. A second assay of the GaAs solutions was carried out  $\geq$ 11 days after EOB (n = 2).

Radioassays involved counting an aliquot of the solutions on ORTEC HPGe detectors (ORTEC-AMETEK@-Oak Ridge, TN; relative efficiencies of 10-30%). The aliquot was diluted with 0.1 N HCl to 3 mL in a plastic vial and positioned on a shelf located 15 cm from the face of the detector. Dead times ranged from 5-9% and 9-22.6% for initial and decayed time points, respectively. A NIST traceable standard containing a mixture of nuclides with emission lines covering the range 59 to 2000 keV was used for calibration. Additionally, a NIST traceable Eu-152 standard (using 344, 779, and 1408 keV gamma rays) was used to verify energies and efficiencies. The acceptance criteria are as follows: the deviation of activity is  $\leq$  4% from the standard value. The peak position deviation is less than 0.5 keV. Both a mixed gamma calibration standard and an Eu-152 standard were prepared and counted in the same geometry as the experimental sample. GammaVision-32 software (AMETEK; version 6.01) was used for detector calibration, spectra acquisition and processing.

Gamma ray energies, branching ratios, and half-lives of the nuclides were obtained from the National Nuclear Data Center (NNDC, **Table 2**)<sup>[51]</sup>. The measured activities of these radionuclides were decay corrected to EOB; the cross section values were calculated using the activation equation for isotope production with protons<sup>[52,53]</sup>.

The beam current was calculated from the <sup>22</sup>Na activity produced in the aluminum foils using cross section data for the <sup>27</sup>Al(p, 2p3n)<sup>22</sup>Na reaction available from the literature.<sup>[46]</sup> Uncertainty in the measured cross sections was determined by propagation of uncertainty in the individual values. Uncertainties in the measurements were as follows: target thickness 2% (both GaAs and Al foil), counting/detector efficiency (3-4%), beam current (5-7%), and pipetting/volumetric dilutions ( $\leq$  1-2%). Uncertainty in calculated energy values take into account the uncertainty of the incident Linac beam energy ( $\pm$  0.1 MeV;  $\sim$ 0.1%), and thickness of the water gaps ( $\pm$  2%). Degrading the energy results in a higher uncertainty in the calculated proton beam energy compared to tuning the Linac to a known, lower incident energy.

## 2.3. <sup>72</sup>Se production targets

### 2.3.1. *Target design and irradiation parameters*

For large scale production, a high-purity (99.999%) GaAs disk (d x h = 3.0" x 0.020" or 76.2 mm x 0.508 mm; American Elements, Los Angeles, CA) was laser cut to 2.375" (6.0325 cm) diameter and isolated in an aluminum capsule (**Figure 3**). The capsule consisted of an aluminum ring (d = 2.750"; 69.85 mm) with a machined window (thickness = 0.080"; 2.032 mm). This arrangement formed a pocket where the GaAs disk was placed. The other window (0.020"; 0.508 mm) was laser-beam welded in a helium atmosphere (EB Industries, Farmingdale, NY). The target was irradiated for 116.5 h (4.85 d) at a calculated proton energy range of 105.4 $\rightarrow$ 104.2 MeV with an average current of 136  $\mu$ A, yielding a total accumulated charge of 15,883.8  $\mu$ Ah (**Table 3**).

Similarly, a high-purity (99.999%) arsenic metal sputtering target (~9.5 g, d x h = 2.375" x 0.032"; 76.2 mm x 0.508 mm from American Elements, Los Angeles, CA) was isolated in an aluminum capsule of a similar design to the GaAs target described above. The As<sup>o</sup> sputtering target was irradiated for 68.9 h (2.87 d) at a calculated proton energy window of 49.5→46.8 MeV with an average current of 163.5 μA, and total accumulated charge of 11,247.8 μAh (**Table 3**). The incident proton energy (117 MeV) was degraded by placing the As<sup>o</sup> target behind a RbCl production target. For both irradiations the instantaneous beam current was measured by a beam current transformer and beam current integrator to measure the current over the entire irradiation in μAh.

### 2.3.2. *Target dissolution and analysis*

Following irradiation, the targets were handled similarly: capsule was cut open, target was removed and transferred to a beaker, and slowly dissolved in 1:1 concentrated nitric acid and 30% H<sub>2</sub>O<sub>2</sub> (~25 mL each for the GaAs target) or 30% H<sub>2</sub>O<sub>2</sub> (~60 mL for the As<sup>o</sup> target). The volume was reduced by evaporation on a hot plate at 80-90 °C (**CAUTION!** Selenium and arsenic are easily volatilized when heated excessively). The remaining GaAs target solution, approximately 25 mL, was quantitatively transferred to a 250 mL volumetric flask using 0.1M HNO<sub>3</sub>, brought up to volume, and three aliquots were taken for analysis by HPGe. After dissolving the arsenic target slowly in 30% H<sub>2</sub>O<sub>2</sub>, 14.5M NH<sub>4</sub>OH (42 mL of 28% w/w NH<sub>3</sub>) was added prior to reducing the volume to approximately 25 mL, whereby the solution was quantitatively transferred to a 250 mL volumetric flask with 0.1M NH<sub>4</sub>OH, brought up to volume, and three aliquots taken for analysis by HPGe.

## 3. Results and Discussion

### 3.1. *Cross-Section Measurements*

#### 3.1.1. *Choice of the target material*

During irradiation the targets were cooled by a forced water system requiring isolation of the target material. Therefore, the cross-section measurement foil and aluminum monitor foil were hermetically sealed in an aluminum can. This press foil design results in reduced heat conductance and thus increased target temperatures due to the imperfect contact between the layers (target window, Al monitoring foil, and cross section measurement foil). Hence, thermal stability was the main parameter that governed the choice of material. Easily obtained, commercially available arsenic containing materials (i.e., InAs, GaAs, AlAs, and As<sup>o</sup>) with suitable thermal properties were identified as possible target materials. The latter three were selected for evaluation by TGA based on their thermal conductivity and higher abundance of arsenic (**Table 4**).

Gallium arsenide and aluminum arsenide were found to be stable at high temperatures of up to 1000 °C. The GaAs was stable up to 1000 °C, which is in agreement with the literature<sup>[54]</sup>. Two weight loss changes were observed in the AlAs TGA thermal curve. The first from 175-225 °C likely corresponds to the loss of unbound water (~1.5%). The second was observed from 325-425 °C likely due to the loss of bound water (~4% loss) and not sublimation of arsenic. AlAs was determined to be thermally stable up to 1000 °C but requires annealing prior to irradiation. There are no literature reports on the thermal decomposition of AlAs however this material may decompose similarly to GaAs. Elemental arsenic was stable up to ~450 °C, at which point it sublimed. A 100% weight loss was observed from 450-550 °C, which is consistent with literature reports<sup>[55]</sup>.

#### 3.1.2. *Target design, irradiation parameters, and foil dissolution*

Both the GaAs and Al foils were sufficiently thin, 0.005" (0.127 mm) and 0.001" (0.0254 mm), so that proton energy degradation across the thickness of the foil was considered negligible. Using the typical variability of the BLIP beamline's incident energy (± 0.1 MeV) the uncertainty of the incident energy was propagated through the foils. Uncertainty of the beam varied by 0.1-0.3 MeV for high and lower energy targets, respectively. Ultimately the uncertainty values were rounded to ± 1 MeV to be conservative. GaAs foils were very brittle and in some instances were recovered in large pieces from the bolted aluminum cans. The fractures may have occurred upon can opening as this was done remotely with hot-cell manipulators. The beam current on the GaAs targets was determined to be 18-38 μA based on the Al monitor foils assay.

Dissolution of the GaAs in concentrated nitric acid and 30% H<sub>2</sub>O<sub>2</sub> (1:1) was rapid and exothermic. It is advisable to add each in small amounts and in sequence, repeating as needed until dissolved, while stirring to better control the reaction. Gamma spectroscopy assays were carried out within one day, and at 11 days post-irradiation to determine the production of short- and long-lived radionuclides, such as <sup>73</sup>Se, and <sup>72,75</sup>Se, respectively.

### 3.1.3. Production of radioselenium (<sup>72/75</sup>Se)

The <sup>72</sup>Se activity can be quantified directly using the gamma emission at 45.9 keV (57.2%), however, the gamma ray of its daughter <sup>72</sup>As (E<sub>γ</sub>—834 keV; 81%) was used for analysis. The target solution was assayed for <sup>72</sup>Se/<sup>72</sup>As quantification using the 834 keV gamma emission of <sup>72</sup>As 11 days after EOB to ensure activity of directly-produced <sup>72</sup>As was negligible ( $\geq 10$  half-lives) and that <sup>72</sup>Se/<sup>72</sup>As were in secular equilibrium. Experimental data reported by Mushtaq et al. and results from this work are compiled in **Figure 2**<sup>[14]</sup>. The data obtained in this work completes the bell-shaped form typical for excitation functions of <sup>75</sup>As(p, 4n)<sup>72</sup>Se and <sup>75</sup>As(p, n)<sup>75</sup>Se nuclear reactions, for which no experimental data above 45.2 MeV had previously been reported.

The experimental data agrees with the theoretical data generated by TALYS 1.4 and EMPIRE 3.1 (Rivoli) codes (**Figure 2**) in that the maximum cross section value for <sup>72</sup>Se occurs at a proton energy around 45 MeV (TALYS) to 50 MeV (EMPIRE). However, the experimental data demonstrates a difference of a factor of two at the cross-section maximum at 50-55 MeV (103 mb experimental vs. 50 mb theoretical)<sup>[14]</sup>.

Selenium-75 is coproduced over the entire energy range shown in **Figure 2**, with lower production rates above 50 MeV. Excitation function for the <sup>75</sup>As(p, n)<sup>75</sup>Se reaction reaches a maximum of ~900 mb centered at 11 MeV<sup>[14,39,40]</sup>. Cross section values decrease from 26 mb to 15 mb from 52 to 105 MeV. Theoretical calculations yielded values close to experimental at proton energies  $\leq 30$  MeV, and under-predicted at higher proton energies<sup>[31]</sup>.

## 3.2. Production Targets

### 3.2.1. Gallium arsenide target

The choice of materials for production was governed by the same criteria as described above for cross section measurements. Additionally, the difficulty level of chemical processing and abundance of arsenic in the target material were considered. Irradiation of a GaAs target was initially carried out mainly due its high thermal stability and existing experience with foils dissolution. Upon opening the capsule it was observed that the GaAs target material was reduced to a powder. The GaAs target was likely reduced to powder by mechanical stress exerted by the pulsed beam at BLIP. The target station is located 30 feet underwater, which creates 1 atmosphere of additional pressure on the target window and may have been a contributing factor to the observed stress on the target.

After dissolution, volumetric dilutions, and sampling (n = 3), it was determined that  $3.8 \pm 0.1$  GBq ( $102 \pm 3$  mCi) of <sup>72</sup>Se and  $0.207 \pm 0.007$  GBq ( $5.6 \pm 2$  mCi) of <sup>75</sup>Se were produced at EOB, which is in excellent agreement, 93% and 94% of theoretical, respectively. The theoretical yield was calculated by dividing the target into 18 equal layers and determining the expected beam energy within each layer using LETCalc<sup>[49]</sup>. The activity produced in each layer was calculated from inputting the average expected energy within each layer into a polynomial fit of the experimental nuclear cross section values obtained from 52-105 MeV. The rates of production of <sup>72</sup>Se and <sup>75</sup>Se were  $0.084 \pm 0.002$  GBq/ $\mu$ A ( $2.27 \pm 0.07$  mCi/ $\mu$ A) and  $0.055 \pm 0.002$  GBq/ $\mu$ A ( $1.49 \pm 0.05$  mCi/ $\mu$ A), respectively, for the GaAs target (<sup>72</sup>Se/<sup>75</sup>Se ratio of 1.53) at 105.4→104.2 MeV. These rates are lower than (3.9x and 140x) the previously reported <sup>72</sup>Se and <sup>75</sup>Se production values of 0.328 GBq/ $\mu$ A (8.9 mCi/ $\mu$ A) and 7.7 GBq/ $\mu$ A (208.0 mCi/ $\mu$ A) when a sodium bromide target was irradiated at LANL however, the <sup>72</sup>Se/<sup>75</sup>Se ratio is ~36 times higher, 1.55 vs. 0.043<sup>[22]</sup>.

### 3.2.2. Arsenic metal target

To simplify chemical processing and increase the production of <sup>72</sup>Se, an arsenic metal target was irradiated. Arsenic metal has a similar density and thermal conductivity to GaAs however, it decomposes at a much lower temperature 450-550 °C vs.  $\geq 1000$  °C. After irradiation, the As<sup>0</sup> target was removed mostly intact in a similar

manner to the GaAs target above. An EOB yield of  $13.80 \pm 0.30$  GBq ( $373.4 \pm 8$  mCi) of  $^{72}\text{Se}$ , and  $0.74 \pm 0.03$  GBq ( $20.1 \pm 0.7$  mCi) of  $^{75}\text{Se}$  were calculated from this irradiation. Experimental results are 22.3%, and 56.5% of theoretical. Theoretical values were calculated to be 62 GBq (1.676 Ci) of  $^{72}\text{Se}$  and 1.31 GBq (35.4 mCi) of  $^{75}\text{Se}$  based on measured cross sections (calculated as described for the GaAs target above), respectively. The rates of production of  $^{72}\text{Se}$  and  $^{75}\text{Se}$  were  $0.400 \pm .009$  GBq/ $\mu\text{A}$  ( $10.8 \pm 0.2$  mCi/ $\mu\text{A}$ ) and  $0.276 \pm 0.010$  MBq/ $\mu\text{A}$  ( $7.5 \pm 0.3$  mCi/ $\mu\text{A}$ ) for the  $\text{As}^\circ$  target ( $^{72}\text{Se}/^{75}\text{Se}$  ratio of 1.45) at a calculated energy of 49.5→46.8 MeV. Production rates for this target are slightly higher (1.22x) for  $^{72}\text{Se}$  and lower (27.9x) for  $^{75}\text{Se}$  than those previously reported by LANL, while the  $^{72}\text{Se}/^{75}\text{Se}$  ratio is similar to the GaAs target, 1.45 vs. 1.55<sup>[22]</sup>.

The 22.3% lower than theoretical  $^{72}\text{Se}$  production yield can be explained by the fact that energy on the As target may have been lower than desired for maximum production. This can be attributed to the uncertainty in the density of the RbCl targets located upstream of the As target. In the energy propagation calculations, the density value for RbCl was assumed to be 2.2 g/cm<sup>3</sup>, corresponding to the RbCl being almost entirely molten in the beam. However, the actual extent of melting in the RbCl targets is unknown. We have determined experimentally that the density of a pressed RbCl target prior to irradiation varies between 2.67 and 2.74 g/cm<sup>3</sup>. The beam energy range for the arsenic target falls from 49.5→46.8 MeV for a RbCl density of 2.2 g/cm<sup>3</sup> to 45.4→42.1 MeV for a RbCl density of 2.68 g/cm<sup>3</sup> and 43.1→39.7 MeV for a RbCl density of 2.74 g/cm<sup>3</sup>. Thus we hypothesize that the RbCl target may not have melted during this irradiation. A dedicated irradiation using degraders with a known density could improve the  $^{72}\text{Se}$  yield.

## 4. Conclusion

Excitation functions for  $^{75}\text{As}(p, xn)^{72}\text{Se}$  in the 52-105 MeV energy range revealed a cross-section maximum of  $103 \pm 9$  mb at  $52 \pm 1$  MeV. After these measurements the routine production of substantial quantities of  $^{72}\text{Se}$  for  $^{72}\text{As}$  production through irradiation of arsenic-containing targets at medium to high energy were determined. Tens of GBq (hundreds of millicuries) of  $^{72}\text{Se}$  could be produced at the BLIP using a GaAs or  $\text{As}^\circ$  target. Future work will include the irradiation of an  $\text{As}^\circ$  target within an optimal proton energy window of 45-60 MeV, development of a chemical process to separate  $^{72}\text{Se}$  from the bulk target material, and packaging of the recovered  $^{72}\text{Se}$  into an easy-to-use generator system in an effort to distribute  $^{72}\text{As}$  as a PET imaging agent at sites remote from the production facility.

*Acknowledgments.* This study was supported by funding provided by the Department of Energy, Office of Nuclear Physics, subprogram Production of High Specific Activity (DE-ST001020) and Brookhaven National Laboratory Isotope LDRD/Program Development (YN0100000). Trainee support is acknowledged from the National Science Foundation under IGERT award DGE-0965983 (M.D. Gott and T.E. Phelps) and the Department of Energy Office of Science Graduate Student Research (SCGSR) award DE-AC05-06OR23100 in 2014 (M. D. Gott) and 2015 (T.E. Phelps). The authors would also like to thank the Center for Functional Nanomaterials for its material analysis infrastructure related to thermal gravimetric analysis. A special thanks to Don Elliott from the instrumentation division at BNL for laser cutting GaAs targets, and the BLIP operator, TPL operators, quality assurance manager, and engineer (Jason Nalepa, Lisa Muench, Slawko Kurzak, Jack Eng, and Christian Cullen) involved with this project.



## References

- 1 Herzog, H., Rösch, F., Stöcklin, G., Lueders, C., Qaim, S.M., and Feinendegen, L.E.: Measurement of Pharmacokinetics of Yttrium-86 Radiopharmaceuticals with PET and Radiation Dose Calculation of Analogous Yttrium-90 Radiotherapeutics. *Journal of Nuclear Medicine* **34**, 2222-2226 (1993).
- 2 Nayak, T.K. and Brechbiel, M.W.: Radioimmunoimaging with Longer-Lived Positron-Emitting Radionuclides: Potentials and Challenges. *Bioconjugate Chemistry* **20**, 825-841 (2009).
- 3 Sweet, W.H. and Brownell, G.L.: Localization of intracranial lesions by scanning with positron-emitting arsenic. *Journal of the American Medical Association* **157**, 1183-1188 (1955).
- 4 Emran, A., Hosain, F., Spencer, R.P., and Kolstad, K.S.: Synthesis and biodistribution of radioarsenic labeled dimethylarsinothiols: Derivatives of penicillamine and mercaptoethanol. *International Journal of Nuclear Medicine and Biology* **11**, 259-261 (1984).
- 5 Hosain, F., Emran, A., Spencer, R.P., and Clampitt, K.S.: Synthesis of radioarsenic labeled dimethylchloroarsine for derivation of a new group of radiopharmaceuticals. *The International Journal of Applied Radiation and Isotopes* **33**, 1477-1478 (1982).
- 6 Lindgren, A., Vahter, M., and Dencker, L.: Autoradiographic studies on the distribution of arsenic in mice and hamsters administered  $^{74}\text{As}$ -arsenite or -arsenate. *Acta Pharmacologica et Toxicologica* **51**, 253-265 (1982).
- 7 Jennewein, M., Schmidt, A., Novgorodov, A.F., Qaim S.M., and Rösch, F.: A no-carrier-added  $^{72}\text{Se}/^{72}\text{As}$  radionuclide generator based on distillation. *Radiochimica Acta* **92**, 245-249 (2004).
- 8 Jennewein, M., Qaim Syed, M., Kulkarni, P.V., Mason, R.P., Hermanne, A., and Rösch, F.: A no-carrier-added  $^{72}\text{Se}/^{72}\text{As}$  radionuclide generator based on solid phase extraction. *Radiochimica Acta* **93**, 579-583 (2005).
- 9 Maki, Y. and Murakami, Y.: The separation of arsenic-77 in a carrier-free state from the parent nuclide germanium-77 by a thin-layer chromatographic method. *Journal of Radioanalytical Chemistry* **22**, 5-12 (1974).
- 10 Gott, M.D., DeGraffenreid, A.J., Feng, Y., Phipps, M.D., Wycoff, D.E., Embree, M.F., Cutler, C.S., Ketring, A.R., and Jurisson, S.S.: chromatographic separation of germanium and arsenic for the production of high purity  $^{77}\text{As}$ . *Journal of Chromatography. A* **1441**, 68-74 (2016).
- 11 Chattopadhyay, S., Pal, S., Vimalnath, K.V., and Das, M.K.: A versatile technique for radiochemical separation of medically useful no-carrier-added (nca) radioarsenic from irradiated germanium oxide targets. *Applied Radiation and Isotopes* **65**, 1202-1207 (2007).
- 12 Bokhari, T.H., Ahmad, M., and Khan, I.U.: Separation of no-carrier-added arsenic-77 from neutron irradiated germanium. *Radiochimica Acta* **97**, 503-506 (2009).
- 13 Jennewein, M., Qaim, S.M., Hermanne, A., Jahn, M., Tsyganov, E., Slavine, N., Seliounine, S., Antich, P.A., Kulkarni, P.V., Thorpe, P.E., Mason, R.P., and Rosch, F.: A new method for radiochemical separation of arsenic from irradiated germanium oxide. *Applied Radiation and Isotopes* **63**, 343-351 (2005).
- 14 Mushtaq, A., Qaim, S.M., and Stöcklin, G.: Production of  $^{73}\text{Se}$  via (p, 3n) and (d, 4n) reactions on arsenic. *Applied Radiation and Isotopes* **39**, 1085-1091 (1988).
- 15 Ellison, P.A., Barnhart, T.E., Engle, J.W., Nickles, R.J., and DeJesus, O.T.: Production and chemical isolation procedure of positron-emitting isotopes of arsenic for environmental and medical applications. *AIP Conference Proceedings* **1509**, 135-140 (2012).
- 16 Takács, S., Takács, M.P., Ditrói, F., Aikawa, M., Haba, H., and Komori, Y.: Activation cross sections of longer-lived radionuclides produced in germanium by alpha particle irradiation. *Nuclear Instruments and Methods in Physics Research Section B: Beam Interactions with Materials and Atoms* **383**, 213-226 (2016).
- 17 Ismail, M.: Measurement and analysis of the excitation function for alpha-induced reactions on Ga and Sb isotopes. *Physical Review C* **41**, 87-108 (1990).
- 18 Mushtaq, A. and Qaim, S.M.: Excitation functions of  $\alpha$ - and  $^3\text{He}$ -particle induced nuclear reactions on natural germanium: Evaluation of production routes for  $^{73}\text{Se}$ . *Radiochimica Acta* **50**, 27 (1990).
- 19 Spahn, I., Steyn, G.F., Nortier, F.M., Coenen, H.H., and Qaim, S.M.: Excitation functions of  $^{\text{nat}}\text{Ge}(p,xn)^{71,72,73,74}\text{As}$  reactions up to 100 MeV with a focus on the production of  $^{72}\text{As}$  for medical and  $^{73}\text{As}$  for environmental studies. *Applied Radiation and Isotopes* **65**, 1057-1064 (2007).

- 20 Shehata, M.M., Scholten, B., Spahn, I., Coenen, H.H., and Qaim, S.M.: Separation of radioarsenic from irradiated germanium oxide targets for the production of  $^{71}\text{As}$  and  $^{72}\text{As}$ . *Journal of Radioanalytical and Nuclear Chemistry* **287**, 435-442 (2010).
- 21 Ellison, P.A., Barnhart, T.E., Chen, F., Hong, H., Zhang, Y., Theuer, C.P., Cai, W., Nickles, R.J., and DeJesus, O.T.: High yield production and radiochemical isolation of isotopically pure arsenic-72 and novel radioarsenic labeling strategies for the development of theranostic radiopharmaceuticals. *Bioconjugate Chemistry* **27**, 179-188 (2016).
- 22 Ballard, B., Wycoff, D., Birnbaum, E.R., John, K.D., Lenz, J.W., Jurisson, S.S., Cutler, C.S., Nortier, F.M., Taylor, W.A., and Fassbender, M.E.: Selenium-72 formation via  $^{nat}\text{Br}(p,x)$  induced by 100 MeV protons: Steps towards a novel  $^{72}\text{Se}/^{72}\text{As}$  generator system. *Applied Radiation and Isotopes* **70**, 595-601 (2012).
- 23 Ballard, B., Nortier, M.F., Birnbaum, E.R., John, K.D., Phillips, D.R., and Fassbender, M.E.: Radioarsenic from a portable  $^{72}\text{Se}/^{72}\text{As}$  generator: A current perspective. *Current Radiopharmaceuticals* **5**, 264-270 (2012).
- 24 Jurisson, S.S., Wycoff, D.E., DeGraffenreid, A., Embree, M.F., Ketring, A.R., Cutler, C.S., Fassbender, M.E., and Ballard, B.: Separation methods for high specific activity radioarsenic. *AIP Conference Proceedings* **1509**, 215-217 (2012).
- 25 Wycoff, D.E., Gott, M.D., DeGraffenreid, A.J., Morrow, R.P., Sisay, N., Embree, M.F., Ballard, B., Fassbender, M.E., Cutler, C.S., Ketring, A.R., and Jurisson, S.S.: Chromatographic separation of selenium and arsenic: A potential  $^{72}\text{Se}/^{72}\text{As}$  generator. *Journal of Chromatography A* **1340**, 109-114 (2014).
- 26 Phillips, D.R., Moody, D.C., Taylor, W.A., Segura, N.J., and Pate, B.D.: Electrolytic separation of selenium isotopes from proton irradiated RbBr targets. *Applied Radiation and Isotopes* **38**, 521-525 (1987).
- 27 Miller, D.A., Grant, M., Erdal, B.R., Whipple, R.E., and O'Brien, H.A.: Nuclear spallation as a mechanism for radioisotope production: Cross sections for selected nuclides. *Journal of Radioanalytical and Nuclear Chemistry* **123**, 643-653 (1988).
- 28 Dmitriev, P.P., Molin, G.A., Konstantinov, I.O., Krasnov, N.N., and Panarii, M.V.: Yields of Se-72 and Se-75 in nuclear reactions with protons, deuterons, and  $\alpha$ -particles. *Soviet Atomic Energy* **34**, 499-500 (1973).
- 29 Amiel, S.: Reactions of alpha particles with germanium-70 and zinc-70. *Physical Review* **116**, 415-417 (1959).
- 30 Calboreanu, A., Salagean, O., Pencea, C., Zimmer, K.W., and Ciocanel, A.: Formation and decay of the compound nucleus in alpha induced reaction on  $^{70}\text{Ge}$ . *Revue Roumaine de Physique* **32**, 725-731 (1987).
- 31 Brodovitch, J.C., Hogan, J.J., and Burns, K.I.: The pre-equilibrium statistical model: Comparison of calculation with two (p, xn) reactions. *Journal of Inorganic and Nuclear Chemistry* **38**, 1581-1586 (1976).
- 32 Röhm, H.F. and Münzel, H.: Excitation functions for deuteron reactions with  $^{75}\text{As}$ . *Journal of Inorganic and Nuclear Chemistry* **34**, 1773-1784 (1972).
- 33 Church, L.B. and Caretto, A.A.: Study of (xp,xn) Reactions at 400 MeV. *Physical Review* **178**, 1732-1742 (1969).
- 34 Grütter, A.: Cross sections for reactions with 593 and 540 MeV protons in aluminium, arsenic, bromine, rubidium and yttrium. *The International Journal of Applied Radiation and Isotopes* **33**, 725-732 (1982).
- 35 Blessing, G., Lavi, N., Hashimoto, K., and Qaim, S.M.: Thermochromatographic separation of radioselenium from irradiated  $\text{Cu}_3\text{As}$  target: Production of no-carrier added  $^{75}\text{Se}$ . *Radiochimica Acta* **65**, 93-98 (1994).
- 36 Blessing, G., Lavi, N., and Qaim, S.M.: Production of  $^{73}\text{Se}$  via the  $^{70}\text{Ge}(\alpha, n)$ -process using high current target materials. *Applied Radiation and Isotopes* **43**, 455-461 (1992).
- 37 Otuka, N. and Takács, S.: Definitions of radioisotope thick target yields. *Radiochimica Acta* **103**, 1-6 (2015).
- 38 Nozaki, T., Itoh, Y., and Ogawa, K.: Yield of  $^{73}\text{Se}$  for various reactions and its chemical processing. *International Journal of Applied Radiation and Isotopes* **30**, 595-599 (1979).
- 39 Levkovskij, V.N.: Middle mass nuclides (A=40-100) activation cross sections by medium energy (E=10-50 MeV) protons and  $\alpha$ -particles (Experiments and Systematics). Inter Vesi, Moscow (1991).
- 40 Johnson, C.H., Trail, C.C., and Galonsky, A.: Thresholds for (xp, xn) reactions on 26 intermediate-weight nuclei. *Physical Review* **136**, B1719-B1729 (1964).
- 41 Qaim, S.M., Sudár, S., Scholten, B., Koning, A.J., and Coenen, H.H.: Evaluation of excitation functions of  $^{100}\text{Mo}(p,d+pn)^{99}\text{Mo}$  and  $^{100}\text{Mo}(p,2n)^{99m}\text{Tc}$  reactions: Estimation of long-lived Tc-impurity and its implication on the specific activity of cyclotron-produced  $^{99m}\text{Tc}$ . *Applied Radiation and Isotopes* **85**, 101-113 (2014).

- 42 Coenen Heinz, H., Gee Antony, D., Adam, M., Antoni, G., Cutler Cathy, S., Fujibayashi, Y., Jeong Jae, M., Mach Robert, H., Mindt Thomas, L., Pike Victor, W., and Windhorst Albert, D.: International Consensus Radiochemistry Nomenclature Guidelines. *Radiochimica Acta* **0**, (2018).
- 43 Herman, M., Capote, R., Carlson, B.V., Obložinský, P., Sin, M., Trkov, A., Wienke, H., and Zerkin, V.: EMPIRE: Nuclear Reaction Model Code System for Data Evaluation. *Nuclear Data Sheets* **108**, 2655-2715 (2007).
- 44 Koning, A.J., Hilaire, S., and Duijvestijn, M.C.: TALYS: Home. <http://www.talys.eu/>
- 45 Medvedev, D.G., Mausner, L.F., Meinken, G.E., Kurczak, S.O., Schnakenberg, H., Dodge, C.J., Korach, E.M., and Srivastava, S.C.: Development of a large scale production of  $^{67}\text{Cu}$  from  $^{68}\text{Zn}$  at the high energy proton accelerator: closing the  $^{68}\text{Zn}$  cycle. *Applied Radiation and Isotopes* **70**, 423-429 (2012).
- 46 Takacs, S., Qaim, S.M., Tarkanyi, F.T., Obložinsky, P., Gul, K., Hermanne, A., Mustafa, M.G., Nortier, F.M., Scholten, B., Shubin, Y., Zhuang, Y.: Monitor Reactions 2017. [https://www-nds.iaea.org/medical/monitor\\_reactions.html](https://www-nds.iaea.org/medical/monitor_reactions.html)
- 47 Titarenko, Y.E., Borovlev, S.P., Butko, M.A., Zhivun, V.M., Pavlov, K.V., Rogov, V.I., Titarenko, A.Y., Tikhonov, R.S., Florya, S.N., and Koldobskiy, A.B.: Cross sections for monitor reactions  $^{27}\text{Al}((p, x)^{24}\text{Na}$ ,  $^{27}\text{Al}(p, x)^{22}\text{Na}$ , and  $^{27}\text{Al}(p, x)^7\text{Be}$  at proton energies in the range 0.04–2.6 GeV. *Physics of Atomic Nuclei* **74**, 507 (2011).
- 48 Michel, R., Bodemann, R., Busemann, H., Daunke, R., Gloris, M., Lange, H.J., Klug, B., Krins, A., Leya, I., Lüpke, M., Neumann, S., Reinhardt, H., Schnatz-Büttgen, M., Herpers, U., Schiekel, T., Sudbrock, F., Holmqvist, B., Condé, H., Malmberg, P., Suter, M., Dittrich-Hannen, B., Kubik, P.W., Synal, H.A., and Filges, D.: Cross sections for the production of residual nuclides by low- and medium-energy protons from the target elements C, N, O, Mg, Al, Si, Ca, Ti, V, Mn, Fe, Co, Ni, Cu, Sr, Y, Zr, Nb, Ba and Au. *Nuclear Instruments and Methods in Physics Research Section B* **129**, 153-193 (1997).
- 49 Zajic, V.: Energy vs. LET Range calculator version 1.24. <http://tvdg10.phy.bnl.gov/LETCalc.html>.
- 50 Ziegler, J.F. and Biersack, J.P.: The Stopping and Range of Ions in Matter. <http://www.srim.org/>.
- 51 Pritychenko, B.: National Nuclear Data Center (NNDC). <https://www.nndc.bnl.gov/>
- 52 Loveland, W.: *Modern Nuclear Chemistry*. (John Wiley & Sons, Inc., Hoboken, New Jersey, 2006).
- 53 Choppin, G.R., Liljenzin, J.-O., and Rydberg, J.: Chapter 15 - Production of Radionuclides, in *Radiochemistry and Nuclear Chemistry (Third Edition)*, edited by Rydberg, G.R.C.-O.L. Butterworth-Heinemann, Woburn, 2002, pp. 388-414.
- 54 Millea, M.F. and Kyser, D.F.: Thermal decomposition of gallium arsenide. *Journal of Applied Physics* **36**, 308-313 (1965).
- 55 Yang, H.-C., Seo, Y.-C., Kim, J.-H., Park, H.-H., and Kang, Y.: Vaporization characteristics of heavy metal compounds at elevated temperatures. *Korean Journal of Chemical Engineering* **11**, 232-238 (1994).

**Table 1.** Cross-section data for proton-induced, selenium yielding nuclear reactions for the 52 to 105 MeV energy range.

Energy (MeV)*	$^{75}\text{As}(p, 4n)^{72}\text{Se}$ Measured cross section $\pm 1 \sigma$ (mb)	$^{75}\text{As}(p, n)^{75}\text{Se}$ Measured cross section $\pm 1 \sigma$ (mb)
52 $\pm$ 1	103 $\pm$ 9	26 $\pm$ 3
63 $\pm$ 1	79 $\pm$ 6	24 $\pm$ 2
76 $\pm$ 1	46 $\pm$ 4	22 $\pm$ 2
86 $\pm$ 1	41 $\pm$ 3	23 $\pm$ 3
99 $\pm$ 1	29 $\pm$ 2	18 $\pm$ 2
105 $\pm$ 1	25 $\pm$ 2	15 $\pm$ 2

\*Propagated Variance: a  $\pm$  0.1 MeV uncertainty in the incident beam energy will propagate to a higher number as lower energies are reached.

**Table 2.** Summary of the nuclear properties of the various radionuclides of arsenic, selenium, and sodium produced from irradiated materials<sup>46</sup>.

Radionuclide	Half-life	$E_\gamma$ in keV (% abundance)*
$^{72}\text{As}$	26.0 h	834 (81)
$^{72}\text{Se}$	8.4 d	46 (57.2); 834 (81) <sup>†</sup>
$^{75}\text{Se}$	119.8 d	136 (58.5)
$^{22}\text{Na}$	2.6 y	1275 (99.9)
$^{24}\text{Na}$	15 h	1369 (100)

\*Gamma emission(s) used for quantification

<sup>†</sup> 831 keV when in equilibrium with  $^{72}\text{As}$

**Table 3.** Summary of large scale irradiation experiments.

Target	Target (d x h, mass)	Energy through target (MeV)	Total accum. charge ( $\mu\text{Ah}$ )	$^{72}\text{Se}$ yield EOB GBq $\pm 1 \sigma$ (mCi)	$^{72}\text{Se}$ theor. yield EOB GBq (mCi)	$^{75}\text{Se}$ yield EOB GBq $\pm 1 \sigma$ (mCi)	$^{75}\text{Se}$ theor. yield EOB GBq (mCi)
GaAs	2.375" x 0.020", 7.7 g (60.325 mm x 0.508 mm)	105.4-104.2	15,883.8	3.8 $\pm$ 0.1 (102 $\pm$ 3)	4.06 (109.7)	0.207 $\pm$ 0.007 (5.6 $\pm$ 0.2)	0.22 (6.04)
As $^{\circ}$	2.375" x 0.032", 9.5 g (60.325 mm x 0.8128 mm)	49.5-46.8	11,247.8	13.80 $\pm$ 0.30 (373 $\pm$ 8)	62.0 (1676.1)	0.74 $\pm$ 0.03 (20.1 $\pm$ 0.7)	1.31 (35.4)

**Table 4.** Physical properties of GaAs, AlAs, and As $^{\circ}$ .

Material	GaAs	AlAs	As $^{\circ}$
Density (g/cm $^3$ )	5.31	3.81	5.78
Thermal conductivity (W $\times$ cm $^{-1}\times$ C $^{-1}$ )	0.55	0.91	0.50
Melting Point ( $^{\circ}\text{C}$ )	1240	1740	871*
TGA Measured decomp. temp. ( $^{\circ}\text{C}$ )	$\geq$ 1000	$\geq$ 1000	450
Mass of arsenic (%)	51.8	73.5	100

\* Arsenic sublimates at 615  $^{\circ}\text{C}$

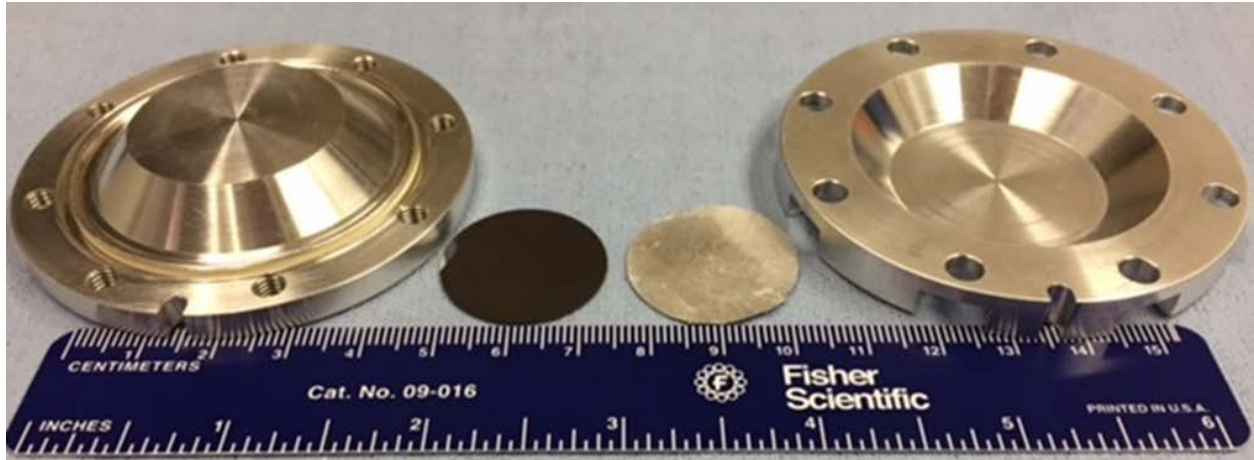


**Figure 1.** Aluminum bolted target can with a GaAs wafer and aluminum foil. Bottom-half (downstream) of target can (left), GaAs wafer (left-middle), aluminum foil (right-middle), and interior of the top-half (right) for cross section measurements.

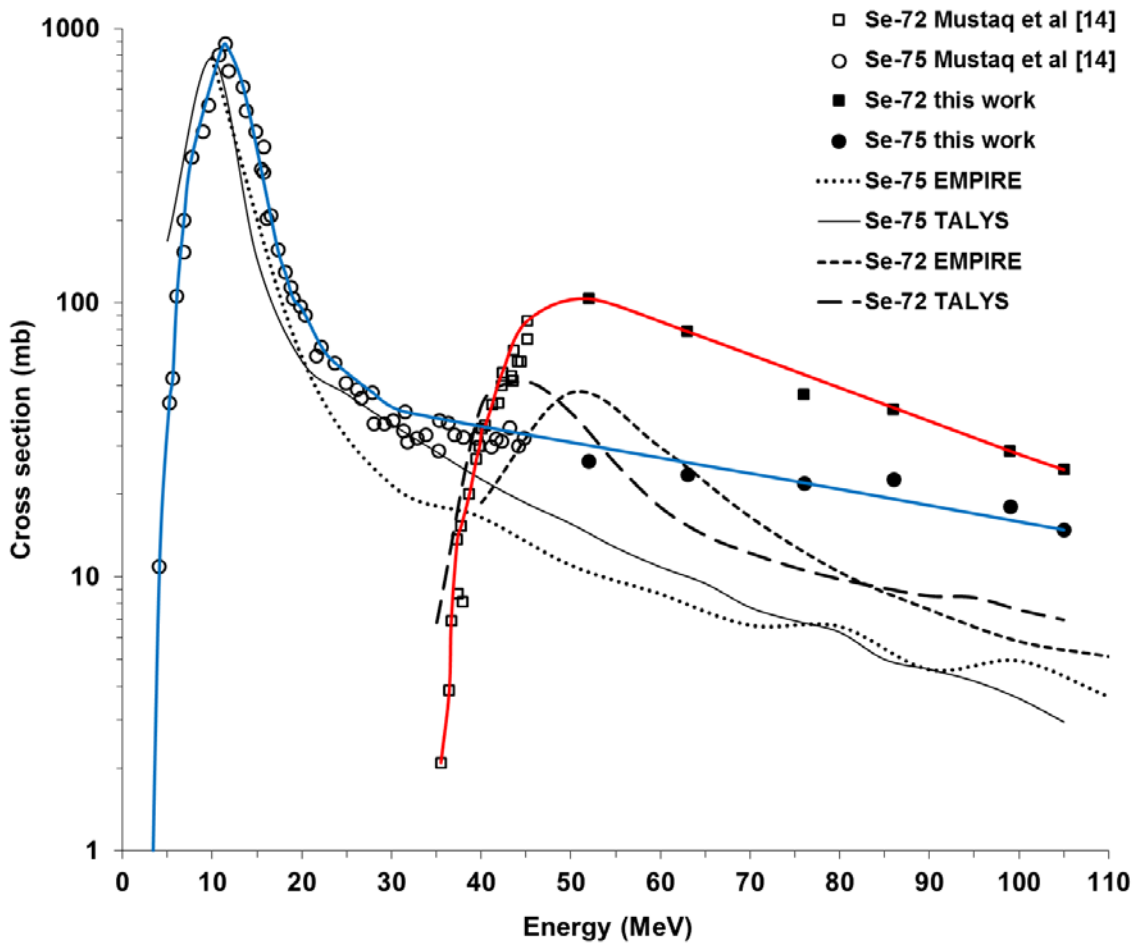


**Figure 2.** Excitation functions of  $^{75}\text{As}(p, 4n)^{72}\text{Se}$ , and  $^{75}\text{As}(p, n)^{75}\text{Se}$  nuclear reactions<sup>14</sup>. The colored lines are to guide the eye.



**Figure 3.** Production target components (from left to right): aluminum window, aluminum can body with machined counter-bore, and arsenic metal sputtering target (d x h = 2.375" x 0.032"; 60.325 mm x 0.8128 mm).

